Fall 10-27-2021

Multi-valued Solutions for the Equation of Motion, Darcy-Jordan Model, as a Cauchy Problem: A Shocking Event

Chandler Shimp

MULTI-VALUED SOLUTIONS FOR THE EQUATION OF MOTION, DARCY-JORDAN MODEL, AS A CAUCHY PROBLEM: A SHOCKING EVENT

by

Chandler Leighanne Shimp

A Thesis
Submitted to the Graduate School,
the College of Arts and Sciences
and the School of Mathematics and Natural Sciences
of The University of Southern Mississippi
in Partial Fulfillment of the Requirements
for the Degree of Master of Science

Approved by:

Dr. James Lambers, Committee Chair
Dr. C. S. Chen
Dr. Haiyan Tian

December 2021

ABSTRACT

Shocks are physical phenomenon that occur quite often around us. In this thesis we examine the occurrence of shocks in finite amplitude acoustic waves from a numerical perspective. These waves, or jump discontinuities, yield ill-behaved solutions when solved numerically. This study takes on the challenge of finding both single- and multi-valued solutions.

The previously unsolved problem in this study is the representation of the Equation of Motion (EoM) in the form of the Darcy-Jordan model (DJM) and expressed as a dimensionless IVP Cauchy problem. Prior attempts to solve have resulted only in implicit solutions or explicit solutions with certain initial conditions.

The approach taken in this study is the development of a hybrid algorithm combining the reliability of the Bisection Method and the efficiency of the Secant method. The developed algorithm is coded in MATLAB.

ACKNOWLEDGMENTS

For my deceased beloveds, Carlene A. McKinney and Joseph M. Shimp, RIP.

As this is my first paper of relevant substance, I want to thank Dr. James Lambers, Dr. C. S. Chen, and Dr. Haiyan Tian for your time, questions, and advice while serving on my committee.

Additional thanks to Dr. Lambers because this would not work without you and your willingness to go the extra mile.

Finally, a special thank you to my loving family (Papa Sandy, Nana Debbie, Martin V., and Izzy) for emotional support and encouragement throughout my years. I am forever grateful.

TABLE OF CONTENTS

LIST OF ILLUSTRATIONS

Figure

NOTATION AND GLOSSARY

General Usage and Terminology

The notation chosen in this thesis represents fairly standard mathematical and computational usage. In many cases these fields tend to use different preferred notation to indicate the same concept, and these have been reconciled to the extent possible, given the interdisciplinary nature of the material. Many specific variables have been chosen to match their usage in the primary source used for this text. This source is listed [1] in the bibliography. The blackboard fonts are used to denote standard sets of numbers: $\mathbb{R}$ for the field of real numbers, $\mathbb{C}$ for the complex field, $\mathbb{Z}$ for the integers, and $\mathbb{Q}$ for the rationals.

Chapter 1

INTRODUCTION

1.1 Introduction

Mathematics is the foundation of human understanding of the physical world. This claim is clear once one observes some physical cause-and-effect relationship. A physical phenomenon occurs, and theoretical physics attempts to describe it analytically. It is not until the numerical mathematician formalizes an algorithm to produce a full solution that we can totally understand this phenomenon. That is exactly what this thesis does.

By analyzing physically applicable solutions to the one-dimensional equation of motion deemed the "damped Riemann equation", we produce the first ever numerical solution to a problem with gradient catastrophe. Prior to this thesis, solutions were limited in that they were either implicit or explicit only with strict initial conditions. Therefore, a need exists for a new algorithm to solve the observation of wave overturning, or shocks. This thesis will make use of one of these explicit solutions, with Lorentzian initial conditions, to test the created algorithm. The challenge presented is due to instances of multi-valued solutions. The developed algorithm will successfully find explicit solutions for both multi- and single-valued positions.

In chapter one and chapter two, this thesis will give proper background knowledge to understand the relevant results of the primary source, allowing the reader to understand the importance of this work. That includes discussing the equation of motion, its representation as a Cauchy problem, and information from the analytical solutions. Then, in chapter three, we will discuss the formation of a new algorithm, which is capable of finding an accurate solution. In the final two chapters, we will look at results of the initial-value problem in question using the new algorithm and discuss future implications.

1.2 The Equation of Motion

Equations of motion (EoMs) are equations that express physical behaviors in terms of motion as a function of time. Consider tossing a ball and watching it fall back down.

This can be studied as one function of motion or two separate functions, where one describes the upward motion and the other describes the downward motion. Equations of motion are applied in instances with uniform acceleration or uniform retardation (decreasing) to estimate the velocity at some point in time other than zero. This makes it possible to find the velocity, acceleration, displacement, and more.

In this study we examine the EoM in one direction for finite-amplitude acoustic waves in relaxing and dual-phased materials. This is represented by the partial differential equation

$$u_t + (v_0 + \sigma u)u_x + \lambda u = 0, \tag{1.1}$$

where v_0, σ, and λ are constants such that $v_0 \neq 0$, $\sigma > 0$, and $\lambda > 0$. Appearing as early as 1962, this equation has been seen in several models for wave propagation. For example, it is used in modeling waves in fluids with a single internal degree of freedom as well as propagation in a gas that admits a single relaxation time, and wherein the internal energy is characterized by two temperatures [**?**, 2]. Finally, and most relevant to this thesis, it appears in the simulations for acoustic wave propagation in dusty gases where the thermal and momentum relaxation times are equivalent [1].

1.3 Darcy-Jordan Model

For the sake of this analysis, our interest in this equation is its application to shocks in solitary waves. Before that connection can be made, we must consider (1.1) in terms of the "damped Riemann equation", denoted this since the special case, $\lambda = 0$, has long been known as the Riemann equation. The Darcy-Jordan Model (DJM) with finite amplitude is given by the weakly linear PDE with dimensionless variables,

$$\Delta^2\phi - \phi_{tt} - \delta\phi_t = \epsilon\delta_t \left[|\nabla\phi|^2 + (\beta - 1)(\phi_t)^2\right]. \tag{1.2}$$

Here, $\phi = \phi(x, y, z, t)$ is scalar velocity potential. The multiplier for nonlinearity is

$$\beta = \begin{cases} (\gamma + 1)/2 & \text{gases} \\ 1 + B/(2 + A) & \text{liquids} \end{cases},$$

where $\gamma \in \left(1, \frac{5}{3}\right]$ is the ratio of specific heats presumed to conduct as a perfect gas, $\frac{B}{A}$ is the parameter of nonlinearity, $\epsilon \propto \frac{1}{C_0}$ is the mach number, $C_0 > 0$ is the speed of sound in this undisturbed fluid, and $\delta \propto X^v/K$ is the dimensionless Darcy coefficient, where t $X \in (0, 1)$ and $K > 0$ represent, respectively, the porosity and permeability of the solid, and $v > 0$ is the kinematic viscosity of the fluid. This is derived from

the assumptions $\epsilon \ll 1$ and $\delta \sim O(\epsilon)$, neglecting the nonlinear terms of $O(\epsilon^2)$ [1]. Considering only the particular one-dimensional expression of (1.2) , we have the form

$$\phi_{xx} - \phi_{tt} - \delta\phi_t = \epsilon\partial_t \left[(\phi_x)^2 + (\beta - 1)(\phi_t)^2\right], \tag{1.3}$$

or in other terms,

$$(\partial_x - \partial_t)(\partial_x + \partial_t)\phi - \delta\phi_t = \epsilon\partial_t \left[(\phi_x)^2 + (\beta - 1)(\phi_t)^2\right]. \tag{1.4}$$

Paying attention only to right-running waves and one-dimensional propagation, we have the damped-Riemann equation with Darcy coefficients,

$$u_t + (1 + \epsilon\beta u)u_x + \frac{1}{2}\delta u = 0. \tag{1.5}$$

Now that we have iterated the origin of this equation, the next chapter will dive deeper into different forms of this equation.

Chapter 2

BACKGROUND

2.1 Cauchy Problem Representation

We must examine the Cauchy problem for (1.5) for different initial conditions. Formulated by Jordan, the dimensionless initial-value problem (IVP), known as the Cauchy problem, is

$$u_t + (1 + \epsilon\beta u)u_x + \frac{1}{2}\delta u = 0, \quad x \in \mathbb{R}, \quad t > 0 \tag{2.1}$$

$$u(x, 0) = u_0(x), \quad x \in \mathbb{R}. \tag{2.2}$$

We impose $u_0(x)$ as a bounded pulse, continuous and positive on the entire real number line. We require that $A_0 = \int_{-\infty}^{\infty} u_0(x)dx$. Here, $u_0(x) \to 0$, as $x \to \pm\infty$ is appropriately rapid so that $A_0 > 0$, meaning that the area beneath is finite.

Taking the obvious approach for this kind of Cauchy problem and applying the method of characteristics to (2.1), (2.2), the exact result is given as the equation of focus for the remainder of this analysis,

$$u(x, t) = u_0(\xi)\exp(-\delta t/2) \tag{2.3}$$

$$x - t - \xi = (\alpha^*)^{-1}u_0(\xi)g(t) \tag{2.4}$$

Note that $\xi = \xi(x, t)$ is the wave variable,

$$g(t) = 1 - \exp(-\delta t/2),$$

and $\alpha^* = \frac{\delta}{2\epsilon\beta}$. The critical amplitude for acceleration waves under DJM is denoted by $\alpha^* \in (0, 1)$.

2.2 Gradient Catastrophe

The hyperbolic and nonlinear nature of (2.1), (2.2) produce an initial-value problem with complicated solutions. That is, nevermind that our $u_0(x)$ is of class $C^0(\mathbb{R})$, or smoother, the solution to (2.1), (2.2) "blows up" at time t^*. The function used to describe shock is denoted

$$u_x(x, t) = \frac{u_0'(\xi)\exp(-\delta t/2)}{1 + u_0'(\xi)g(t)/\alpha^*}. \tag{2.5}$$

[1] This is the key complexity to this study, known as "gradient catastrophe" or finite-time wave overturning at time $t = t^*$. If t^* is positive and real, we can physically interpret this catastrophe as a shock wave with formation beginning at time t^*. This is believed, and we will show, to be a multi-valued solution. Given the root equation, refer to (2.4), it appears that catastrophe is a bifurcation such that a single root becomes multiple roots.

Finally, before our numerical analysis begins, let us consider some physically relevant examples of shock waves. These propagating waves often occur, based on the notion that matter is compressible, as significant disruptions in some compressible channel. Examples of such a common occasion often go unnoticed in a human's daily surroundings. For a natural example, they stem from such phenomena as volcanic eruptions, earthquakes, or lightning. Synthetically, they derive from sonic booms or chemical explosions. One very common example of propagating shock waves occurs in traffic when cars together known as "ghost jams" and "traffic shocks" [5].

2.3 Analyzing Initial and Boundary Conditions in Prior Attempts

Attempts have been made to find the multi-valued solution of equations (2.1), (2.2), but prior to the work of Jordan there existed only one physically relevant solution. This solution was only represented in implicit form.

2.3.1 Sinusoidal IC

Prior attempts to solve this problem include the insertion of sinusoidal (having the form of a sine curve) initial conditions. That is,

$$u_0(\xi) = \sin(k\xi), \tag{2.6}$$

where $k > 0$ is a dimensionless wavenumber (the spatial frequency of a wave). Clearly, in this case, $|u_x| = \infty$ when $k|\cos(k\xi)|g(t^*) = \alpha^*$. Since the maximum of $|\cos(k\xi)|$ is equal to one, then here

$$t^* = \begin{cases} -2\delta^{-1}\ln(1-\alpha^*/k), & \alpha^* < k, \\ \infty, & \alpha^* = k \end{cases}$$

Note that $t^* \in \mathbb{C}$ for $\alpha^* > k$ therefore time gradient catastrophe exists only for $a^* < k$, leaving out much of the physical complexity surrounding this problem. This initial condition resulted in only one physically applicable solution of implicit form.

2.3.2 Lorentzian IC

Jordan produced the first explicit solution to equation (2.1), (2.2) using initial conditions, an algebraic function, called Lorentzian conditions. This initial condition is particularly important as, later in this thesis, it will be used to test the result of the developed algorithm.

First, by recasting the damped Riemann equations as a kinematic system, the resulting constant integral, with respect to time, is equivalent to the classic Riemann equation:

$$\int_{-\infty}^{\infty} u_0(\xi(x,t))\ dx = A_0, \quad t > 0$$

where A_0 is equal to the constant of integration and $\xi = \xi(x,t)$ is the wave variable, as mentioned previously.

The Lorentzian condition begins with letting

$$u_0(\xi) = \frac{\varkappa^2}{\varkappa^2 + \xi^2}, \tag{2.7}$$

where $A_0 = \varkappa\pi$. Substituting this into the system (2.1), (2.2), gives

$$u(x,t) = \varkappa^2 \exp(-\delta t/2)(\varkappa^2 + \xi^2) \tag{2.8}$$

$$\xi^3 - \eta\xi^2 + \varkappa^2\xi + \varkappa^2\left[(\alpha^*)^{-1}g(t) - \eta\right] = 0, \tag{2.9}$$

with $\eta = x - t$. Relevant near the end of this chapter,

$$\Delta(\eta,t) = Q^3(\eta) + R^2(\eta,t),$$

with

$$Q(\eta) = \frac{3\varkappa^2 - \eta^2}{9},$$

and

$$R(\eta,t) = \frac{2\eta^3 - 9\varkappa^2\eta - 27\varkappa^2\left[(\alpha^*) - 1 - g(t) - \eta\right]}{54},$$

and finally letting

$$\kappa^* = \frac{3\sqrt{3}}{8\alpha^*}.$$

Using the same logic explained for the sinusoidal condition,

$$t^* = \begin{cases} -2\delta^{-1}\ln\left(1 - \varkappa/\varkappa^*\right), & \varkappa < \varkappa^*, \\ \infty, & \varkappa = \varkappa^*, \end{cases}$$

with $t^* \in \mathbb{C}$ for $\varkappa > \varkappa^*$, where $\varkappa^*$ is a critical value.

This results in a u versus x profile with a slope bounded for every $t > 0$ ($0 < t < t^*$) if $\varkappa \geq \varkappa^*$ ($\varkappa < \varkappa^*$) showing that the solution profile contains exactly one stationary point, a maximum, with a critical point of $\xi = \bar{\xi}$ where $\bar{\xi} = 0$. The statement that $\varkappa \geq \varkappa^*$ shows that finite-time gradient catastrophe is avoided for the Lorentzian initial condition and that

$$\xi_!(x,t) = S^+(x-t,t) + S^-(x-t,t) + \frac{1}{3}(x-t),$$

where

$$S^{\pm}(\eta,t) = \sqrt[3]{R(\eta,t) \pm \sqrt{\Delta(\eta,t)}}.$$

Using similar logic, with $t \in (0, t^*)$, avoidance applies to the case $\varkappa < \varkappa^*$.

The interesting analysis occurs for $t = t^*$, which as stated is the instant of gradient catastrophe where

$$\eta = \eta_{gc},$$
$$\eta_{gc} = x_{gc} - t^* = (9/8)(\varkappa/\varkappa^*)/\alpha^* = \varkappa\sqrt{3}$$

is the η-coordinate of the point associated with $t = t*$, when gradient catastrophe occurs. It is shown that

$$\xi_!(x_{gc}, t^*) = \frac{1}{3}\eta_{gc} = \frac{3}{8}(\varkappa/\varkappa^*)/\alpha^* = \varkappa/\sqrt{3}$$

is a bifurcation where a single root becomes a root of multiplicity three. Further, it is shown that when $t > t^*$ the quartic equation $\Delta(\eta, t) = 0$ admits exactly two real roots denoted $r_{1,2} = r_{1,2}(t)$. We can conclude that there exist three real roots, with only two of them being equal, to the equation with Lorentzian conditions. Futhermore, the theory of cubic equations suggests that this equation has three unequal roots, which we will denote $\xi_{1,2,3}(x,t)$ when $r_1 < \eta < r_2$. Finally, when $\Delta(\eta,t) > 0$ when $t > t^*$, this equation produces only one real root ($\eta_!(x,t)$). This shows that a shock forms after time $t = t^*$.

While Jordan did find an exact solution for (2.1), (2.2), the analytics to explain this solution are quite complex and not relevant to the remainder of this study. With some mathematical finesse and interpolation, Jordan was able to create a MATLAB graph with (2.8) showcasing multiple solutions.

2.3.3 Symmetric-Exponential Initial Condition

One other explicit solution exists using the function

$$u_0(\xi) = \exp(-\varkappa|\xi|), \tag{2.10}$$

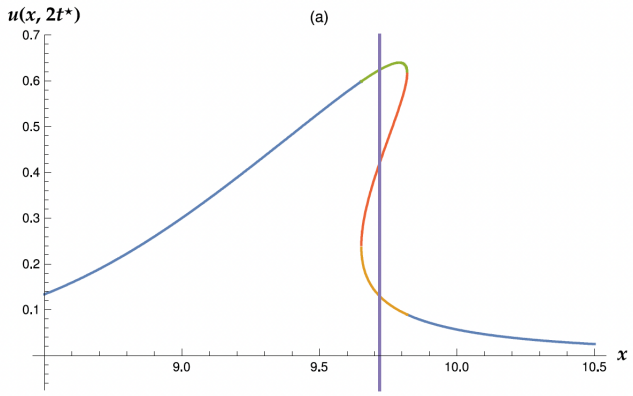

Figure 2.1: Graph for Lorentzian conditions with $t = 2t^*$, $\beta = 1.2$, and $\varepsilon = \delta = 0.1$ showing multi-valuedness approximately $9.6 < x < 9.8$ with shock around 9.7.

sometimes known as Green's function of a Hookean oscillator or as an "even decaying pulse" (Strang). Here, it was found to admit an acceleration wave. The exact multi-valued solution with this initial condition was found to be:

$$u(x,t) = \exp(-\delta t/2)\exp\left[\varkappa \xi_M(x,t)\right], \quad t > 0 \tag{2.11}$$

where ξ_M represents explicit expressions for ξ determined using the "Lambert W-function".

Chapter 3

METHODS

3.1 Intervals of Interest

We were able to determine our interval of interest, or interval $[a, b]$ that we need to use to solve (2.4) using information provided through analytics. The interval of interest occurs along with a discontinuity in the graphing of ξ and x. This gives an idea of which intervals to examine. The case below shows when the solution is actually multi-valued, which can be seen from the fact that the function, F, in the top plot has three roots. On the left is the graph of al roots, ξ on F where F is equation (2.4) with Lorentzian conditions as seen in equation (2.8). On the right is the graph ξ versus x.

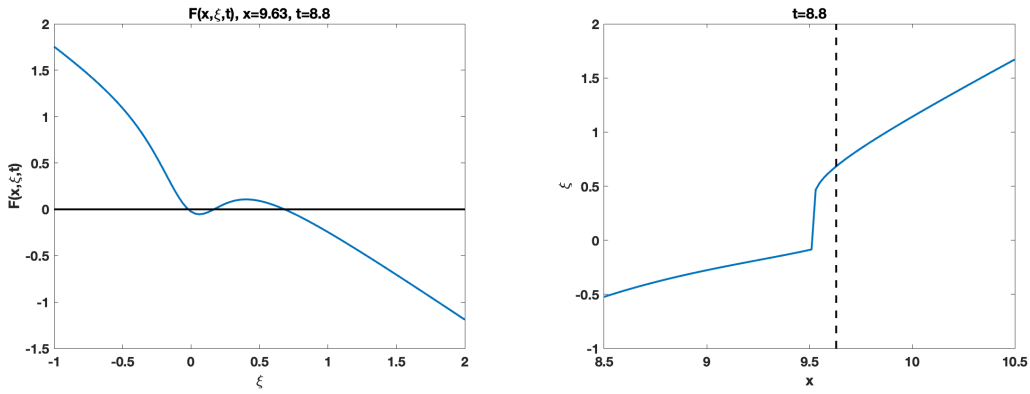

Figure 3.1: These images were created via MATLAB and depend on (2.8).

In the above images we can see that multi-valuedness appears, in the left image, around $-0.25 < \xi < 0.75$. Similarly, in the right of 3.1 there is a discontinuity roughly when $-0.25 < \xi < 0.5$. This suggests that one method to determine an interesting interval would be to use a MATLAB function which detects discontinuities. Additionally, in the plot of ξ and x, the roots appear to "spread out" when the solution is single-valued. This appears to be equivalent to the discontinuity observation, and it is the method used in this computation to determine our interval.

3.2 Algorithm

3.2.1 Algorithm Concept

To find a general solution for (2.1), (2.2), we developed an algorithm combining the efficiency of the Secant method and the accuracy and reliability of bisection. Our goal was to find all possible solutions for $f(x) = 0$ on some interval $[a, b]$ for (2.8), (2.9). Before getting into MATLAB, we should consider the theory behind this algorithm. For the sake of understanding this algorithm, one must understand our subintervals. That is, how they are determined and how they change throughout iterations.

Taking the assumption that there exists reasonable spacing between each of the roots, we divide $[a, b]$ into n equal subintervals. x-values are determined from $a,\ b,\ n$ serving as points on the initial interval with a goal to cover all space between a and b. We then examine each x for a root, ξ for a fixed time, t. That is, we solve $F(\xi) = 0$ for a fixed x and t. Clearly, a change in sign from one x_i to the next would indicate a root, but we do not have the luxury of assuming sign changes from the very beginning. We ensure that each $x-$value in the grid is examined to find all ξ-values that satisfy equation (2.4). This allows a numerical solution for multi-valued roots. Once a sign change from ξ_i to ξ_{i+1} has been spotted we can proceed. In this case i indicates the index variable, $i = 1, 2, 3, \ldots$.

For each x-value, consider some subinterval with a left endpoint ξ_L and a right endpoint ξ_R. We begin by using the secant method with our endpoints as initial guesses. An iteration of bisection is performed if the secant method fails or the result is outside of our interval. That is, we find the midpoint, $\xi_M = (\xi_R + \xi_L)/2$. We know that $f(\xi_L)f(\xi_R) < 0$; therefore, either $f(\xi_L)f(\xi_M) < 0$ or $f(\xi_M)f(\xi_R) < 0$. If $f(\xi_L)f(\xi_M) < 0$, we move on to the interval (ξ_L, ξ_R). Otherwise, $f(\xi_M)f(\xi_R) < 0$ and we use (ξ_M, ξ_R). Once this is complete we use the secant method again. The secant method, which uses a finite difference to approximate the derivative of a function by a secant line through two points, was chosen as the efficient counterpart to bisection's reliability. We use the current endpoints as the initial guesses for this iteration. The iterations of secant method continue, as long as each iterate is in our current interval, until a root is detected. Again, if the secant method fails or produces a result outside of our interval, bisection is used as before to narrow down the location further. Iterations occur between the secant method and bisection until a root is located.

3.2.2 Algorithm Development

MATLAB algorithm development consists of the following parts: define grid points as

a vector of x-values, create of loops to define the end points of each subinterval of x and delegate to the root-finding function, find the root(s) using bisection and the secant method, and finally store them to vector given as the final output. To do this, four functions were created. They will be discussed in chronological order of creation, not to be confused with order of implementation.

First was a more basic function to perform the secant method. This is the last function to be called, so at this point the subinterval of interest is already determined. This function intakes values for r, q, f where $r = \xi_i$ and $q = \xi_{i+1}$ for the most recent ξ-values. If the result of the secant method is successful, the discovered root (ξ) is stored and sent to `rootfinder`. However, if the secant method fails to converge within the interval, a flag is sent to the function `rootfinder`. This separates this function from a typical secant implementation.

The written code `rootfinder` takes care of dictating when to perform bisection and when to perform secant method. As stated this performs the secant method for the correct conditions as stated above. This takes each ξ value found in secant and stores it into an array of ξ-values that is given in the final output. An index i is use to keep up with which x-value we are dealing with.

The `solvepde` function carries perhaps the most difficult portion of the algorithm, keeping up with the changes in intervals. It holds an array of all x-values and an array of all ξ-values, and it ensures that each interval is examined. `Solvepde` calls `rootfinder` once the intervals have been updated.

Finally, the `values` was created to hold the parameters of the PDE we wish to solve. This includes initial values, the initial interval, the number of subintervals, and the number of iterations in the final plot.

Chapter 4

Results

4.1 Testing

As stated, this algorithm was tested using Lorentzian conditions. That is, taking

$$u_0(\xi) = \frac{\varkappa^2}{\varkappa^2 + \xi^2} \tag{4.1}$$

with the following parameters:

- The interval $[a = 8.5, b = 10.5]$
- $\delta = \varepsilon = 0.1$
- $\beta = 1.2$
- $\alpha^* = \frac{\delta}{2\varepsilon\beta}$
- $\varkappa^* = \frac{3\sqrt{3}}{8\alpha^*}$
- $\varkappa = 0.2\varkappa^*$.

Adjusting the number and size of subintervals so that they incorporate all space in the interval of interest, the following input variables produced the best results:

- $N = 100$
- $dt = 0.01$
- $T = 10$
- $n = 200$.

Our results were successful in that multi-valuedness was shown true and roots were detected where expected.

4.2 Solutions

The images below exemplify the behavior of the discovered solution for single and multi-valuedness.

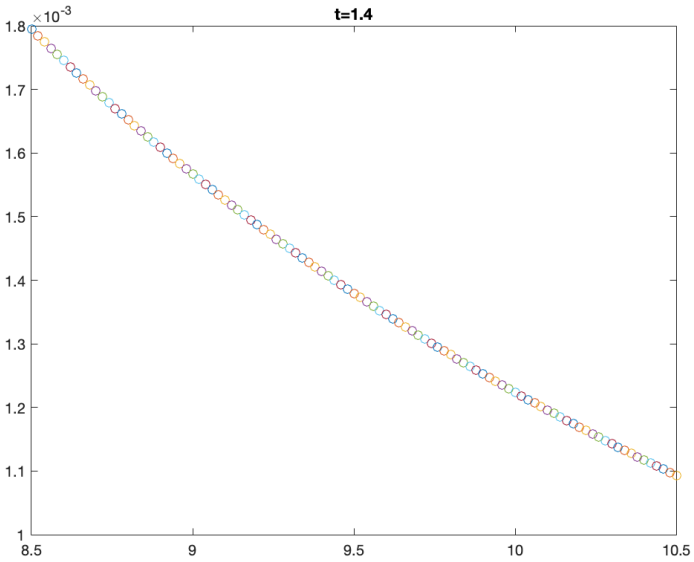

Figure 4.1: At time $t = 1.4$, the code successfully find single-valued roots for each point prior to shock

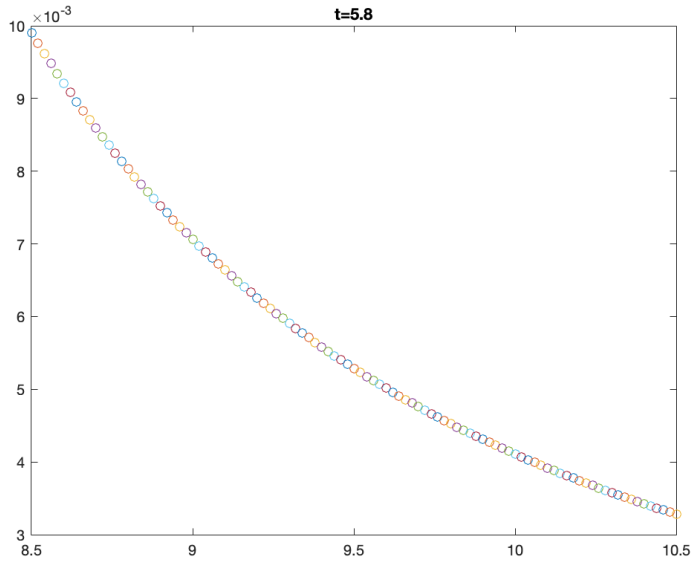

Figure 4.2: We begin to notice the spread in single-valued roots near $t = 5.4$

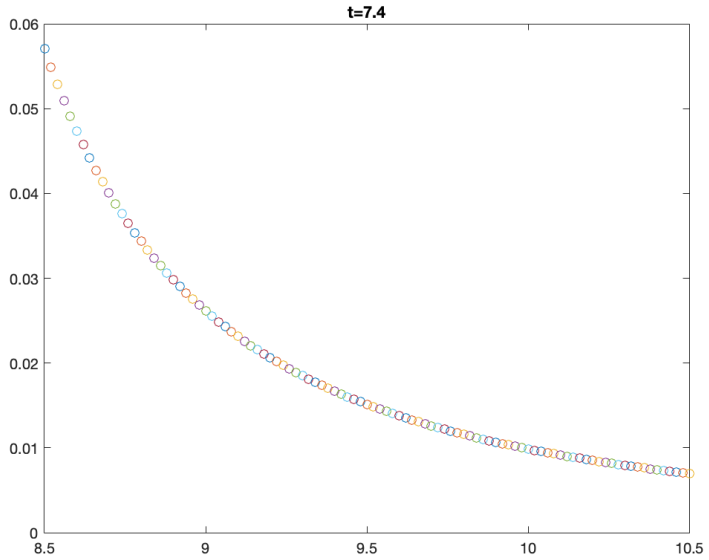

Figure 4.3: The spread space between roots keeps increasing, here we see we are approaching multi-valuedness at time $t = 7.4$

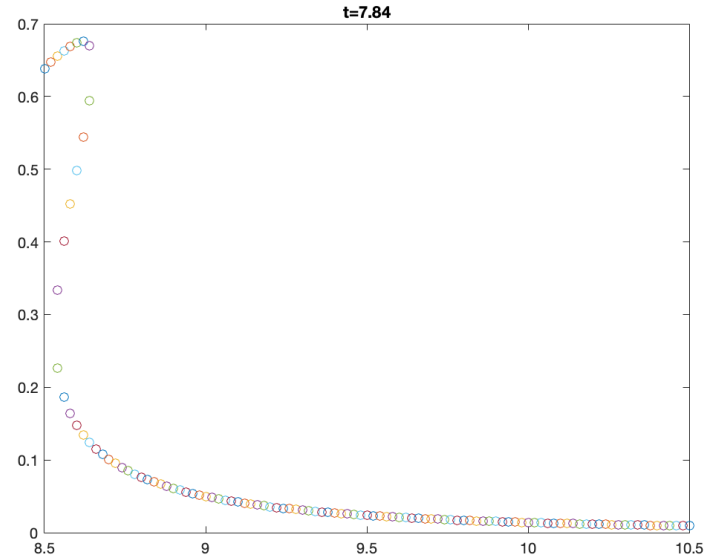

Figure 4.4: At the time $t = 7.84$, multi-valuedness is apparent

Chapter 5

Conclusion

This problem is one step closer to a general solution. We created a new algorithm combining the accuracy of the Bisection method with the efficiency of the Secant method. We chose careful coded instructions to ensure no gaps existed between subintervals. Our results, after a couple of easy parameter adjustments, were as expected and found all physically relevant roots. As mentioned, problems surrounding shocks have many physical applications. More specifically, shock analysis in acoustic traveling waves in fluids in porous materials, has applications in the fields of applied mathematics, fluid dynamics, mechanics, and acoustics.

While multi-valuedness was successfully found for this problem with Lorentzian conditions, the next step is to test the algorithm with other initial conditions, beginning with the aforementioned Symmetric-Exponential conditions. This step is in progress now. Logical steps from here include testing a variety of parameters in order to optimize efficiency, and time was the primary limitation in this study. We worked under the assumption that each interval has at most one root, and it would be particularly interesting to explore that idea further.

Appendix A

MATLAB FUNCTIONS

A.1 MATLAB Functions

Code for `Secant` function:

```
function[x0,flag] = secant(r,q,f)

r1=r;
q1=q;
flag=0;
while abs(f(q)) > 0.000005
    x0=(r*f(q)-q*f(r))/(f(q)-f(r));
    if (x0 < r1) || (x0 > q1)
        flag=1;
        return
    end

    r=q;
    q=x0;

end

x0=q;
```

Code for `rootfinder` function:

```
function [xis] = rootfinder(a,b,f,n)

x=linspace(a,b,n+1);
y= 0*x;
xis=[];

for i=1:n
    y(i)=f(x(i));
end

for i=1:n
    if y(i)*y(i+1)<0
        r=x(i);
        q=x(i+1);
        [xi,flag] = secant(r,q,f);
        while flag
           m=(r+q)/2;
           if f(m)*f(r)<0
               q=m;
           else
               r=m;
           end
            [xi,flag] = secant(r,q,f);
        end
        xis=[xis,xi];
    end

end
```

Code for `solvepde`:

```
function solvepde(a,b,u0,N,dt,T)

delta=0.1;
epsilon=0.1;
g=@(t)(1-exp(-delta*t/2));
beta=1.2;
alphas=delta/(2*epsilon*beta);
dx=(b-a)/N;
x=a:dx:b;
El=zeros(size(x));
Er=zeros(size(x));

for j=1:length(x)
    if j==1
        El(j)=x(1)-dx;
    else
        El(j)=x(j)-dx;
    end
    if j==length(x)
        Er(j)=x(end)+dx;
    else
        Er(j)=x(j)+dx;
    end
end

for n=1:ceil(T/dt)
    t=n*dt;
    for j=1:length(x)
        F=@(xi)(x(j)-t-xi-((alphas)^(-1)*u0(xi)*g(t)));
        ni=(Er(j)-El(j))/dx*100;
        Es = rootfinder(El(j),Er(j),F,ni);
        while isempty(Es)
            m=(El(j)+Er(j))/2;
            r=(Er(j)-El(j))/2;
```

```
            El(j)=m-2*r;
            Er(j)=m+2*r;
            ni=2*ni;
            Es = rootfinder(El(j),Er(j),F,ni);
        end
        if length(Es)>1
            disp('multi-valued!')
        end
        for k=1:length(Es)
            u=u0(Es(k))*exp(-delta*t/2);
            plot(x(j),u,'o')
            hold on
        end

        El(j)=min(Es)-dx;
        Er(j)=max(Es)+dx;
    end
    title(['t=' num2str(t)])
    pause(0.01)
    hold off
    for j=1:length(x)
        Elnew(j)=min(El(max(1,j-10):min(length(x),j+10)));
        Ernew(j)=max(Er(max(1,j-10):min(length(x),j+10)));
    end

    El=Elnew;
    Er=Ernew;

end
```

Values:

```
a=8.5;
b=10.5;
delta=0.1;
epsilon=0.1;
beta=1.2;
alphas=delta/(2*epsilon*beta);
kappas=(3*sqrt(3))/(8*alphas);
k=0.2*kappas;
u0=@(Es)(k^2./(k^2+Es.^2));
N=100;
dt=0.01;
T=7.84;
n=200;
x=linspace(a,b,n+1);
plot(x,u0(x),'o')
pause
solvepde(a,b,u0,N,dt,T)
```

BIBLIOGRAPHY

[1] P.M. Jordan: "Poroacoustic Solitary Waves Under the Unidirectional Darcy-Jordan Model", *Wave Motion* **94** (2020).

[2] D.G. Crighton: *Nonlinear Waves in Aerosols and Dusty Gases in: A. Kluwick (Ed.), Nonlinear Waves in Real Fluids*, (1991), 69-82.

[3] S.I. Soluyan, R.V. Khokhlov: *English Translation: Finite Amplitude Acoustic Waves in a Relaxing Medium*, *Acoust.* **8** (1962), 220-227.

[4] E.Varley, T.G. Rogers: *T*he Propagation of High Frequency, Finite Acceleration Pulses and Shocks in Viscoelastic Materials, (1967), 498-518.

[5] D. Levison: *Shockwaves*, (2021)

[6] "Equations of Motion (Physics)", uploaded by Manocha Aademy, (2018)